

Topological depletions and universal sub-leading scalings across topological phase transitions

Fadi Sun and Jinwu Ye

Department of Physics and Astronomy, Mississippi State University, P. O. Box 5167, Mississippi State, MS, 39762

Department of Physics, Capital Normal University,

Key Laboratory of Terahertz Optoelectronics, Ministry of Education,

and Beijing Advanced Innovation Center for Imaging Technology, Beijing, 100048, China

Kavli Institute of Theoretical Physics, University of California, Santa Barbara, Santa Barbara, CA 93106

(Dated: May 11, 2019)

It remains an open problem if there are universal scaling functions across a topological quantum phase transition (TPT) without an order parameter, but with extended Fermi surfaces (FS). Here, we study a simple system of fermions hopping in a cubic lattice subject to a Weyl type spin-orbit coupling (SOC). As one tunes the SOC parameter at the half filling, the system displays Weyl fermions and also various TPT due to the collision of particle-particle or hole-hole Weyl Fermi Surface (WFS). At the zero temperature, the TPT is found to be a third order one whose critical exponent is determined. We derive the scaling functions of the specific heat, compressibility and magnetic susceptibilities. In contrast to all the previous cases in quantum or topological transitions, although the leading terms are non-universal and cutoff dependent, the sub-leading terms satisfy universal scaling relations. The sub-leading scaling leads to the topological depletions (TD) which show non-analytic and non-Fermi liquid corrections in the quantum critical regime, can be easily distinguished from the analytic leading terms and detected experimentally. One can also form a topological Wilson ratio from the TD of two conserved quantities such as the specific heat and the compressibility. As a byproduct, we also find Type II Weyl fermions appearing as the TPT due to the collision of the extended particle-hole WFS. Experimental realizations and detections in cold atom systems and materials with SOC are discussed.

1. Introduction. It was established that experimental measurable quantities near a quantum phase transition with an order parameter satisfy various universal scaling functions at a finite temperature [1, 2]. In another forefront, topological phases and phase transitions without an order parameter were studied since the experimental observations of the quantum Hall effects [3, 4] and under even more intense investigations after the discovery of topological insulators [5]. It is important to investigate if there are still universal scaling functions across various topological phase transitions without an order parameter. Here, we address this outstanding problem by studying a very simple system of free fermions hopping in a cubic lattice subject to a Weyl type of spin-orbit coupling [6]. Our main results are summarized in the abstract. The experimental motivations of this model from both cold atoms and materials will be discussed in Sec.7.

2. 8 Type I Weyl fermions. The Hamiltonian of fermions hopping in a cubic lattice subject to Weyl type spin-orbit coupling in Fig.1a can be written as

$$H = \sum_k h_i(\mathbf{k})\sigma_i, i = 0, 1, 2, 3 \quad (1)$$

where $\sigma_i = \sigma_0$ is the identity matrix, σ_i are 3 Pauli matrices and $h_0(\mathbf{k}) = -2t(\cos\alpha\cos k_x + \cos\beta\cos k_y + \cos\gamma\cos k_z)$, $h_x(\mathbf{k}) = 2t\sin\alpha\sin k_x$, $h_y(\mathbf{k}) = 2t\sin\beta\sin k_y$, $h_z(\mathbf{k}) = 2t\sin\gamma\sin k_z$. Its two energy bands are $\epsilon_{\pm}(\mathbf{k}) = h_0(\mathbf{k}) \pm h(\mathbf{k})$ where $h(\mathbf{k}) = \sqrt{[h_x(\mathbf{k})]^2 + [h_y(\mathbf{k})]^2 + [h_z(\mathbf{k})]^2}$. At half filling $\mu = 0$, the

particle and hole FS is given by $\epsilon_{\pm}(\mathbf{k}) = 0$. The particle energy is related to that of the hole $\epsilon_+(\vec{k} + \vec{Q}) = -\epsilon_-(\vec{k})$ where $\vec{Q} = (\pi, \pi, \pi)$ is the FS nesting vector which separates the particle FS from the hole FS. It leads to the relation between the particle DOS and that of hole $D_+(\omega) = D_-(-\omega)$ at the half filling $\mu = 0$.

At $(\alpha, \beta, \gamma) = (\pi/2, \pi/2, \pi/2)$, there are 8 Type I Weyl fermions located at $(k_x = 0, \pi, k_y = 0, \pi, k_z = 0, \pi)$ carrying the topological monopole charges $N_3 = \pm 1$ in Fig.1b. It is the inversion symmetry breaking in Eq.1 which leads to their existences. As one tunes the SOC parameters, some or all Weyl fermions will become closed particle or hole Weyl Fermi surface (WFS) which still keep the topological charges $N_3 = \pm 1$ of the Weyl fermions and satisfy $\sum_{i=1}^8 N_{3i} = 0$ during the evolution [4]. How the WFS evolve along the three lines $(\alpha = \beta = \gamma = \theta)$, $(\alpha = \pi/2, \beta = \gamma = \theta)$ and $(\alpha = \beta = \pi/2, \gamma = \theta)$ are shown in Fig.2,3,4 respectively.

3. The third order TPT along $\alpha = \beta = \gamma = \theta$ at zero temperature. There is a TPT driven by the collisions of the 4 WFS where the colliding 4 particle WFS takes a saddle point (cone) geometry near a Von Hove singularity $K_c = 2\pi/3$ and the critical SOC parameter $\theta_c = \pi/3$. When expanding around the VHS $K = K_c + \Delta/\sqrt{3}$ and θ_c , we get the particle energy spectrum:

$$\epsilon_+(\vec{q}) = -[\Delta + aq_x^2 - b(q_y^2 + q_z^2)] \quad (2)$$

where $\vec{k} = \vec{K} + \vec{q}$, $\Delta = \sqrt{3}(\theta_c - \theta)$ is the tuning parameter and $a = 1/2, b = 3/4 + \Delta/4$.

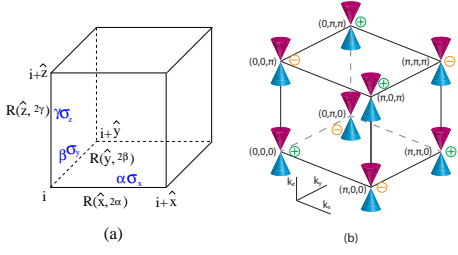


FIG. 1. (a) The non-abelian gauge fields ($\alpha\sigma_x, \beta\sigma_y, \gamma\sigma_z$) are put on the three links in a cubic lattice. (b) The 8 Weyl fermions with the topological charges $N_3 = \pm 1$ at $\alpha = \beta = \gamma = \pi/2$.

The DOS takes the piece-wise form:

$$D(\omega) = \begin{cases} B[\Lambda - \sqrt{\frac{-(\omega+\Delta)}{a}}], & \omega + \Delta < 0 \\ B\Lambda, & \omega + \Delta > 0 \end{cases} \quad (3)$$

where Λ is the momentum cutoff and $B = \frac{1}{(2\pi)^2 b}$. Note the non-analytic depletion in the DOS due to the TPT.

From the DOS, we can evaluate the ground state energy:

$$E \sim \begin{cases} \alpha\Delta^2 + \frac{1}{(2\pi)^2 b} \frac{2}{\sqrt{a}} \frac{2}{15} |\Delta|^{5/2} + \dots, & \Delta < 0 \\ \alpha\Delta^2 + B_0\Delta^3 + \dots, & \Delta > 0 \end{cases} \quad (4)$$

where \dots means analytical terms or higher order non-analytic terms, the α, B_0 are cutoff dependent. Only the leading non-analytic term is cutoff in-dependent and universal.

Plugging the parameters $\Delta = \sqrt{3}(\theta_c - \theta), a = 1/2, b = 3/4 + \Delta/4$ into Eq.4 and taking two derivatives lead to:

$$E''(\theta, \mu = 0) \sim \begin{cases} \alpha + A_0\sqrt{\theta - \theta_c}, & \theta > \theta_c \\ \alpha + B_0(\theta - \theta_c), & \theta < \theta_c \end{cases} \quad (5)$$

where the exponents $\nu_- = 1/2, \nu_+ = 1$ are universal and the coefficient $A_0 = 0.18856$ is cutoff independent and stands for the universal contributions from a single cone in Fig.2. While B_0 is not universal and cut-off dependent. At the half filling $\mu = 0$, there are 6 particle and 6 hole WFS colliding at the same time. So in the second derivatives of the total ground state energy: $A = 12A_0 = 2.262$.

We performed numerical calculations on the ground state energy in the BZ (See SM).

$$E''_n(\theta, \mu = 0) \sim \begin{cases} -0.77 + A_n(\theta - \theta_c)^{\nu_+}, & \theta > \theta_c \\ -0.77 + B_n(\theta - \theta_c)^{\nu_-}, & \theta < \theta_c \end{cases} \quad (6)$$

where the numerical exponents $\nu_+ = 0.5 \pm 0.05, \nu_- = 1.0 \pm 0.05$ match the analytical values $\nu_+ = 1/2, \nu_- = 1$ well, the numerical coefficient $A_n = 2.19$ is also very close to the analytical value $A = 2.262$ achieved above.

4. Universal sub-leading scaling functions across the third TPT at a finite T. From Eq.2, intuitively, one can still define the dynamic exponent $z = 2$ with respect to the cone singularity. However, due to the

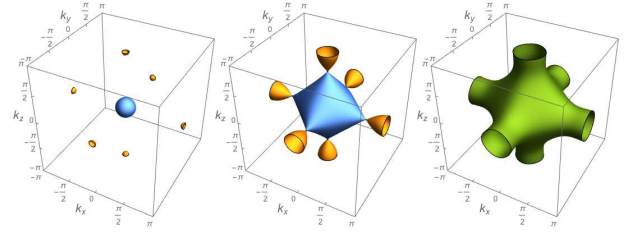


FIG. 2. The particle WFS evolves along $\alpha = \beta = \gamma = \theta$ for $\theta = 4\pi/9, \pi/3, \pi/4$. At the QCP $\theta_c = \pi/3$, the big WFS with $N_3 = 1$ (blue) hits the other 3 small WFS (yellow) with $N_3 = -1$ at 6 Fermi points at $\vec{K}_c = (\pm 2\pi/3, 0, 0), (0, \pm 2\pi/3, 0), (0, 0, \pm 2\pi/3)$. As θ increases further, it becomes a whole (green faucet tap-like) Fermi surface with the total $N_3 = 1 - 1 - 1 - 1 = -2$ charge, so it is a topological non-trivial FS. The hole WFS can be reached by shifting the particle WFS by the FS nesting vector (π, π, π) .

low energy excitations around the WFS on both sides of the TPT, its physical meaning remains to be carefully examined. In the following, we show that it is the subleading terms which satisfy the universal scaling with $z = 2$ and lead to non-analytic therefore non-Fermi liquid corrections to the leading analytic terms.

One can apply the scaling analysis in [7] here to write down the sub-leading scaling functions for the specific heat and the uniform compressibility $\kappa_u = \chi^{00}(\vec{q} \rightarrow 0, \omega = 0)$ for a single particle-particle (or hole-hole) cone in Fig.2:

$$C_v = \frac{\pi^2}{3} B k_B (k_B T) \Lambda - \frac{B k_B (k_B T)^{3/2}}{\sqrt{a}} \Psi_i\left(\frac{|\Delta|}{k_B T}\right) \quad (7)$$

$$\kappa_u = \frac{1}{2} B \Lambda - \frac{B (k_B T)^{1/2}}{\sqrt{a}} \Omega_i\left(\frac{|\Delta|}{k_B T}\right)$$

where $i = 1, 2$ stands for the two sides of the transitions $\Delta < 0$ and $\Delta > 0$ in Fig.2 and Fig.5. Note the first term is the leading term, proportional to the frequency (or energy) cutoff Λ and non-universal. while the second term is the sub-leading term, independent of the frequency (or energy) cutoff Λ and a universal function of the scaling variable $s = \frac{|\Delta|}{k_B T}$. Due to the opposite sign between the two terms, the universal sub-leading term can be interpreted as the topological depletion coming from the TPT.

The general form of the two scaling functions $\Psi_i(x)$ and $\Omega_i(x)$ are evaluated in the SM. Here, we only list the topological depletions in the three limiting regimes in Fig.5 for the specific heat

$$C_v^{TD} = \begin{cases} -\frac{\pi^2}{3} \frac{B}{\sqrt{a}} k_B^2 T \sqrt{|\Delta|}, & \Delta \ll -k_B T \\ -2.88201 \frac{B}{\sqrt{a}} k_B^{5/2} T^{3/2}, & |\Delta| \ll k_B T \\ -\frac{\sqrt{\pi}}{2} \frac{B k_B^{1/2}}{\sqrt{a}} \frac{\Delta^2}{\sqrt{T}} e^{-\frac{\Delta}{k_B T}}, & \Delta \gg k_B T \end{cases} \quad (8)$$

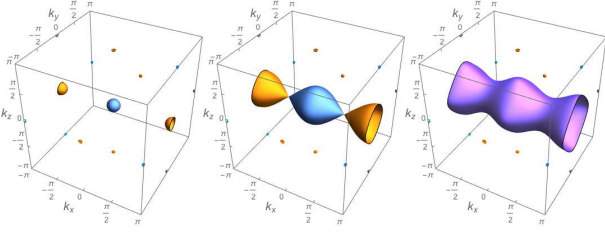


FIG. 3. The particle WFS evolves along $\alpha = \pi/2, \beta = \gamma = \theta$ for $\theta = 4\pi/9, \pi/3, \pi/4$. At $\theta_c = \pi/3$, the WFS with $N_3 = 1$ hits the one with $N_3 = -1$ at the two Fermi points at $\vec{K}_c = (\pm\pi/2, 0, 0)$. As θ decreases further, it becomes a whole Fermi surface (violet vase) with the total $N_3 = 1 - 1 = 0$ charge, so it is topologically trivial FS. There are 4 Weyl fermions remaining intact through the TPT. The hole WFS can be reached by shifting the particle WFS by one of the two FS nesting vectors $(0, \pi, \pi), (\pi, \pi, \pi)$.

and for the uniform compressibility:

$$\kappa_u^{TD} = \begin{cases} -\frac{B}{\sqrt{a}}\sqrt{|\Delta|}, & \Delta \ll -k_B T \\ -0.536077 \frac{B k_B^{1/2} T^{1/2}}{\sqrt{a}}, & |\Delta| \ll k_B T \\ -\frac{\sqrt{\pi} B k_B^{1/2} T^{1/2}}{2\sqrt{a}} e^{-\frac{\Delta}{k_B T}}, & \Delta \gg k_B T \end{cases} \quad (9)$$

One can see both topological depletions are non-analytic only in the QC regime in Fig.5. While, essentially no depletion when $\Delta \gg T$ and a constant $\sqrt{|\Delta|}$ depletion when $-\Delta \gg T$ which can be absorbed to the leading FL contribution anyway. This fact make their experimental detections feasible (see Sec.7).

One can also form the topological Wilson ratio $R_W^{TD} \left(\frac{|\Delta|}{k_B T} \right) = \frac{k_B^2 T \kappa_u^{TD}}{C_v^{TD}}$ whose values in the three regimes are:

$$R_W^{TD} = \begin{cases} 3/\pi^2 & \Delta \ll -k_B T \\ 0.186, & |\Delta| \ll k_B T \\ \left(\frac{k_B T}{\Delta} \right)^2, & \Delta \gg k_B T \end{cases} \quad (10)$$

which is even independent of a and b characterizing the shape of the cone. In fact, it is also independent of how many cones are participating in the TPT, so universal for all the TPTs in Fig.2,3,4.

Due to the $[C_4 \times C_4]_D$ symmetry at $\alpha = \beta = \gamma$, the topological depletions of the magnetic susceptibility $\chi^{xx}(T) = \chi^{yy}(T) = \chi^{zz}(T) = \frac{1}{3}\chi^{00}(T)$ also satisfy the sub-leading scaling Eq.9.

5. The 3rd order TPT along $\alpha = \pi/2, \beta = \gamma = \theta$ and co-existence of four Type I Weyl fermions. At half filling $\mu = 0$, 2 particle WFS and 2 hole WFS collide at the same time at $\vec{K}_c = (\pi/2, 0, 0)$ and $\theta_c = \pi/3$ (Fig.3). The dispersion near $K_c = \pm\pi/2, \theta_c = \pi/3$ can also be written as Eq.2 where $\Delta = \sqrt{3}(\theta_c - \theta), a = 1/2, b = 5/8 - \Delta^2/8$. Using Eq.5, we find $A_0 = 0.2263$,

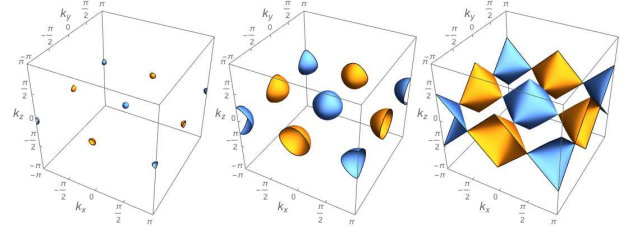


FIG. 4. The particle WFS evolves along $\alpha = \beta = \pi/2, \gamma = \theta$ for $\theta = 4\pi/9, \pi/4, 0$. The TPT happens at the end point $\theta_c = 0$ where it becomes a corner-sharing octahedron. The hole WFS can be reached by shifting the particle WFS by one of the 4 FS nesting vectors $(0, 0, \pi), (\pi, 0, \pi), (0, \pi, \pi), (\pi, \pi, \pi)$. There are also 8 Type II Weyl fermions at $\theta_c = 0$ due to the collision of the particle WFS and the hole WFS.

then the 2 particle WFS and 2 hole WFS contribute to $A = 4A_0 = 0.90$. Similarly, the subleading scaling function in Eq.8 and Eq.9 need also multiply by 4, but the topological Wilson ratio Eq.10 remains identical.

We also performed numerical calculation in the whole BZ and get a similar form as Eq.6 where $A_n = 0.861$ is quite close to the analytic value $A = 4A_0 = 0.90$.

As shown in Fig.3, there are also 4 Type I Weyl fermions located at $(0, 0, \pi), (0, \pi, 0), (\pi, 0, \pi), (\pi, \pi, 0)$ with the anisotropic dispersion $\epsilon_{\pm}^I = \pm\sqrt{q_x^2 + \sin^2\theta(q_y^2 + q_z^2)}$. They remain intact through the TPT, so just act as 4 spectators. Due to its dynamic exponent $z = 1$, their contributions $C_v \sim T^3, \chi_u \sim T^2$ are analytic and subleading to the topological non-analytic depletions in the QC regime due to the third order TPT.

6. The 5th order TPT along the line $\alpha = \beta = \pi/2, \gamma = \theta$ and the 8 Type II Weyl fermions. At half filling $\mu = 0$, all the 4 particle WFS and 4 hole WFS collide at the same time at $\theta_c = 0$ (Fig.4). Near $\vec{K}_c = (\pi/2, 0, 0), \theta_c = 0$, the dispersion can also be written as Eq.2 where $\Delta = -\theta^2/2, a = 1/2, b = 1/2 + \Delta/2$. Note the quadratic dependence of Δ on the SOC tuning parameter θ . Plugging these parameters into Eq.4, we find the transition is a 5th order one with $\frac{d^5 E}{d\theta^5} \sim \frac{8}{\pi^2} \text{sgn}\theta$. Fig.4 dictates that $A = 12A_0 = \frac{96}{\pi^2}$. All the subleading scaling function in Eq.8 and Eq.9 need also be multiplied by 12, but the topological Wilson ratio Eq.10 remains the same.

As shown in Fig.4, in addition to the particle-particle and hole-hole WFS collisions, the particle WFS also collide with the hole WFS at the 8 momenta $(0, 0, \pm\pi/2), (\pi, 0, \pm\pi/2), (\pi, \pi, \pm\pi/2), (0, \pi, \pm\pi/2)$. Such a cone structure between the particle WFS and the hole WFS is nothing but a special case of the type II Weyl fermions discussed in [11]. One Type II Weyl fermion's dispersion at $(0, 0, \pi/2)$ is given by: $\epsilon_{\pm}^{II}(\vec{q}) = -[-q_z \mp \sqrt{q_x^2 + q_y^2}]$ where the \mp corresponds to the particle and hole WFS (see Fig.4). In the Type II

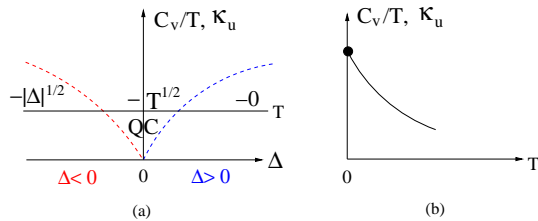


FIG. 5. Experimental signatures of the topological depletions and sub-leading scalings (a) The specific heat C_v/T and the compressibility κ_u at a given T shows a universal non-analytic \sqrt{T} depletion in the quantum critical (QC) regime. (b) The quantum \sqrt{T} cusps in C_v/T and κ_u in the QC regime as T lowers. From the ratio of the coefficients of the \sqrt{T} in the two quantities, one may also measure the universal Topological Wilson ratio R_W^{TD} .

Weyl fermion, both the extended particle and hole WFS add to contribute to a finite DOS $D(\omega) \sim \Lambda^2 - \alpha\omega^2$ with a possible topological depletion in DOS $\sim \alpha\omega^2$, so it is a metallic phase [13]. For tilted Type II Weyl fermions in [11], $\alpha > 0$. While for the straight Type II Weyl fermions in Fig.4, $\alpha = 0$. From the simple scaling analysis, the 8 Type II Weyl fermions with $z = 1$ contribute to the depletion in the specific heat $C_v^D \sim \alpha T^3$ which is subleading to the topological depletion $C_v^D \sim T^{3/2}$ due to the 5th order TPT in the QC regime. In fact, as said above, for the straight Type II Weyl fermions, even the coefficient $\alpha = 0$, so it does not even have a topological depletion.

7. Experimental realizations and detections in cold atoms and materials. The Hamiltonian Eq.1 can be achieved by loading cold atoms in a cubic optical lattice [14–18]. Note that the TPT in Fig.2,3,4 are for non-interacting fermions, they are essentially single particle properties, so the heating issues should be manageable in current cold atom experiments with fermions.

Of course, any experiments are performed at finite temperatures which are controlled by the topological phase transitions at $T = 0$ in Fig.2,3,4. The crossover temperature in Fig.5 can be estimated as $T \sim \Delta \sim t \sim 3nK$ which is easily experimental reachable with the current cooling techniques [20, 21], so the \sqrt{T} quantum cusp behaviors in C_v/T and κ_u , the universal Topological Wilson ratio in Fig.5 can be measured by the specific heat [22, 23], *In-Situ* [24] and the compressibility κ measurements [23]. The change of the FS topology across the TPT in Fig.2,3,4 can be monitored by the momentum resolved interband transitions [25] and the band mapping technique developed in [16].

Type I Weyl fermions have been discovered in several materials [9, 10]. Type II Weyl fermions [11] seem also have been found in a few materials [12]. Topological Lifshitz transitions happen in all these Type I and Type II Weyl fermion materials. Although they may not be de-

scribed precisely by the Hamiltonian Eq.1, they should be in the same topological classes as those in Fig.2,3,4. So the results achieved in this paper should also apply to the Topological Lifshitz transitions in these non-interacting or weakly interacting Type I and Type II Weyl fermion materials.

8. Discussions and Conclusions. Eq.8 and 9 take a similar form to the topological entanglement entropy [26]: $S = \alpha L - \gamma$ where the first term (Area law) is the leading non-universal term proportional to the length between the boundary of the two entangled regimes A and B. While the second term is the sub-leading term, independent of the boundary and universal called topological entanglement entropy $\gamma = \log D$ where D is quantum dimension D (which is a counter-part of the dynamic exponent z here). There is also a relative minus sign between the two terms. This suggests that the form may be a general scaling structure across a TPT.

The quantum subleading scaling behaviors in the specific heat in Eq.8 remind the classical cusp of the specific heat near the finite temperature phase transition of the classical $O(3)$ Heisenberg model [27] $C_v \sim C - b_0 t^{-\alpha}$ where $t = |(T - T_c)/T_c|$, $b_0 > 0$ and $\alpha \sim -0.1$. This cusp has been precisely detected in specific heat experiments. This fact has also been used to determine the Anomalous Hall effect near the finite temperature phase transition in [28]. Here the quantum \sqrt{T} cusp behavior in the QC regime near $T = 0$ in Fig.5 is due to the TPT at $(T = 0, \Delta = 0)$.

The present paper focused on only the half filling case with $\mu = 0$. Our preliminary results away from half filling shows there are new classes of TPT with anisotropic dynamic exponents [29]. Due to the vanishing of DOS at the Type I Weyl fermions, a weak interaction is irrelevant. But due to the extended FS at the Type II Weyl fermions, the particle-particle WFS or hole-hole WFS TPT cone singularity, any weak interaction is relevant. Following Ref.[30–35], it is important to look at the effects of both positive U and negative U .

We thank Yu Yi-Xiang for the early participation of the project and acknowledge AFOSR FA9550-16-1-0412 for the supports. The work at KITP was supported by NSF PHY11-25915.

-
- [1] S. Sachdev and J. Ye, Phys.Rev.Lett. 69, 2411 (1992); A. V. Chubukov, S. Sachdev, and J. Ye, Phys. Rev. B **49**, 11919(1994).
 - [2] S. Sachdev, *Quantum Phase transitions*, (2nd edition, Cambridge University Press, 2011).
 - [3] X.G. Wen and Q. Niu, Phys. Rev. B41, 9377 (1990); Wen, X. G. Quantum Field Theory of Many-body Systems (Oxford University Press, 2004).
 - [4] Volovik, G. E. The Universe in a Helium Droplet (Oxford University Press, USA, 2003).

- [5] M. Z. Hasan and C. L. Kane, *Rev. Mod. Phys.* **82**, 3045 (2010); X. L. Qi and S. C. Zhang, *Rev. Mod. Phys.* **83**, 1057 (2011).
- [6] Shang-Shun Zhang, Jinwu Ye, Wu-Ming Liu, *Phys. Rev. B* **94**, 115121 (2016).
- [7] Fa-Di Sun, Xiao-Lu Yu, Jinwu Ye, Heng Fan, W. M. Liu, *Scientific Reports* **3**, 2119 (2013).
- [8] For a review, see Turner, A. M. & Vishwanath, A. Preprint at <http://arxiv.org/abs/1301.0330> (2013).
- [9] Su-Yang Xu, *et.al*, *NATURE PHYSICS — VOL 11 — SEPTEMBER 2015*; *Science* **349**, 613 (2015); L. X. Yang, *et.al*, *NATURE PHYSICS — VOL 11 — SEPTEMBER 2015*; B. Q. Lv, *et.al*, *NATURE PHYSICS — VOL 11 — SEPTEMBER 2015*.
- [10] Ling Lu, *et.al*, John D. Joannopoulos and Marin Soljacic, *Science* **349**, 622 (2015).
- [11] A.A. Soluyanov, *et.al*, *Nature (London)* **527**, 495 (2015).
- [12] A. Tamai, *et.al* and F. Baumberger, *PHYSICAL REVIEW X* **6**, 031021 (2016).
- [13] We think that the title "Type-II Weyl Semimetals " in Ref.[11] maybe mis-leading, due to th extended particle and hole WFS, Type II Weyl fermions lead to a metal instead of a semi-metal.
- [14] Lianghui Huang, *et.al*, *Nature Physics* **12**, 540-544 (2016).
- [15] Zengming Meng, *et.al*, arXiv:1511.08492.
- [16] Zhan Wu, *et.al*, *Science* **354**, 83-88 (2016).
- [17] Michael L. Wall, *et.al*, *Phys. Rev. Lett.* **116**, 035301 (2016).
- [18] L. F. Livi, *et.al*, *Phys. Rev. Lett.* **117**, 220401 (2016); S. Kolkowitz, *et.al*, arXiv:1608.03854; Fangzhao Alex An, *et.al*, arXiv:1609.09467.
- [19] Nathaniel Q. Burdick, Yijun Tang, and Benjamin L. Lev, *Phys. Rev. X* **6**, 031022 (2016).
- [20] Medley, P., Weld, D. M., Miyake, H., Pritchard, D. E. & Ketterle, W. *Phys. Rev. Lett.* **106**, 195301 (2011).
- [21] Sugawa, S. *et al*, *Nat. Phys.* **7**, 642 (2011).
- [22] Kinast, J. *et al*, *Science* **307**, 1296 (2005).
- [23] Ku, M. J. H. *et al*, *Science* **335**, 563 (2012).
- [24] Gemelke, N., Zhang X., Huang C. L., and Chin, C. *Nature (London)* **460**, 995 (2009).
- [25] Leticia Tarruell, *et.al*, *Nature* **483**, 302-305 (2011).
- [26] M. Levin and X. G. Wen, *Phys. Rev. Lett.* **96**, 110405, (2006); A. Kitaev and J. Preskill, *Phys. Rev. Lett.* **96**, 110404 (2006).
- [27] C. Holm and W. Janke, *J. Phys. A* **27**, 2553 (1994); M. H. Lau and C. Dasgupta, *Phys. Rev. B* **39**, 7212 (1989); M. Kamal and G. Murthy, *Phys. Rev. Lett.* **71**, 1911 (1993).
- [28] J. Ye, Y. B. Kim, A. J. Millis, B. I. Shraiman, P. Majumdar, and Z. Tešanović, *Phys. Rev. Lett.* **83**, 3737 (1999).
- [29] The leading anisotropic dynamic exponents associated with the bosonic analog of the Type II Weyl fermions happen in the Rotated Ferromagnetic Heisenberg model (RFHM) in a longitudinal Zeeman field [31], but not in a transverse field [32].
- [30] Fadi Sun, Jinwu Ye, Wu-Ming Liu, *Phys. Rev. A* **92**, 043609 (2015).
- [31] Fadi Sun, Jinwu Ye, Wu-Ming Liu, arXiv:1502.05338.
- [32] Fadi Sun, Jinwu Ye, Wu-Ming Liu, *Phys. Rev. B* **94**, 024409 (2016).
- [33] Fadi Sun, Jinwu Ye, Wu-Ming Liu, arXiv:1601.01642, to be published.
- [34] Yi-Xiang Yu, Jinwu Ye, Wu-Ming Liu, *Phys. Rev. A* **90**, 053603 (2014).
- [35] Yu Yi-Xiang, Fadi, Sun, Jinwu Ye and Ningfang Song, arXiv:1609.06554.